

# Robust Online Detection in Serially Correlated Directed Network

Miaomiao Yu<sup>a</sup>, Yuhao Zhou<sup>\*b</sup>, and Fugee Tsung<sup>c</sup>

<sup>a</sup>Key Laboratory of Advanced Theory and Application in Statistics and Data Science, MOE, and Academy of Statistics and Interdisciplinary Sciences, East China Normal University, Shanghai, China

<sup>b</sup>Department of Statistics and Operations Research, University of North Carolina at Chapel Hill, Chapel Hill, NC 27599, USA

<sup>c</sup>Department of Industrial Engineering and Decision Analytics, Hong Kong University of Science and Technology, Kowloon, Hong Kong.

**Abstract:** With the increasing complexity of the production process, the diversity of data types contributes to the urgency of developing the network monitoring technology. This paper mainly focuses on an online algorithm to detect the serially correlated directed network robustly and sensitively. Firstly, a transition probability matrix is considered here to overcome the double correlation of primary data. Furthermore, since the sum of each row of the transition probability matrix is one, it also standardizes data that facilitates subsequent modeling. Then we extend the spring-length-based method to the multivariate case and propose an adaptive cumulative sum (CUSUM) control chart on the strength of a weighted statistic to monitor directed networks. The novel approach only assumes that the process observation is associated with nearby points without any parametric time series models, which should be coincided with the fact. Simulation results and a real example of metro transportation demonstrate the superiority of our design.

**Keywords:** Directed Network; Serially Correlation; CUSUM control chart; Weighted Statistic; Transition probability

## 1 Introduction

Statistical process control (SPC) technology is one of the most prevalent tools to monitor the quality of manufactured products and is encountered in almost every field, such as company operation

analysis (Han et al., 2020), semiconductor manufacturing (Xiang et al., 2021) and human genetics (Zou et al., 2020). In the era of big data, it faces tremendous challenges, especially in the sparse development of strategies for monitoring networks and/or graphics data that is widespread in diverse scenarios (Crane and Dempsey, 2018; Asikainen et al., 2020; Zhang et al., 2021). In this paper, we focus on the online monitoring problem of a serially correlated directed network (e.g. transportation system), in which the feature of correlation undermines the assumption of conventional monitoring technologies and leads to its unreliable performance (Qiu and Xie, 2021).

The motivation of our paper comes from the real example of metro traffic detection. The urban metro transportation system, with its characteristics of reliability, high capacity and environmental friendliness, has become a popular style of transportation to relieve the traffic pressure in modern big cities. It is well known that metro lines are naturally unstable because of uncertain disturbances, such as system abnormality, inadequate driver/passenger action, and so on (Lin and Sheu, 2010; Li et al., 2016). And any deviation with respect to the nominal schedule of a given train will be amplified with time, and consequently, the operation of other trains will be disturbed (Campion et al., 1985). Thus it is important to check whether a certain line is in control (IC) and the negative results may remind operators to adjust schedule in time to avoid traffic jams and property losses. In this case, there exist two major problems. On the one hand, the metro traffic problem is a directed network that can be converted into a square matrix and few methods are currently available to detect the matrix. On the other hand, high-frequency traffic data does not satisfy the assumption of independence which may kill the algorithmic efficiency. What is worse, the existence of double correlation in this case brings more challenges to algorithm stability. More specifically, the serial correlation of the number of people transferred from station A to station B is caused by the autocorrelations of traffic load and transition probability as shown in Figure 1 - 2.

In addition, there are many other examples from other domains, such as risk management in financial markets (Yu et al., 2018). In real application, we often take advantage of the changes of the topological structure in financial networks to predict the incoming financial crisis. It has been found that the above topological structures are usually associated with the co-movements of the oil prices. So, the daily spot prices of crude oil are as a way to measure the risks of financial networks. Then this directed network shows the influence on the time-dependent cross-correlations of prices at adjacent time points between pairs of regions. Similar applications include the online

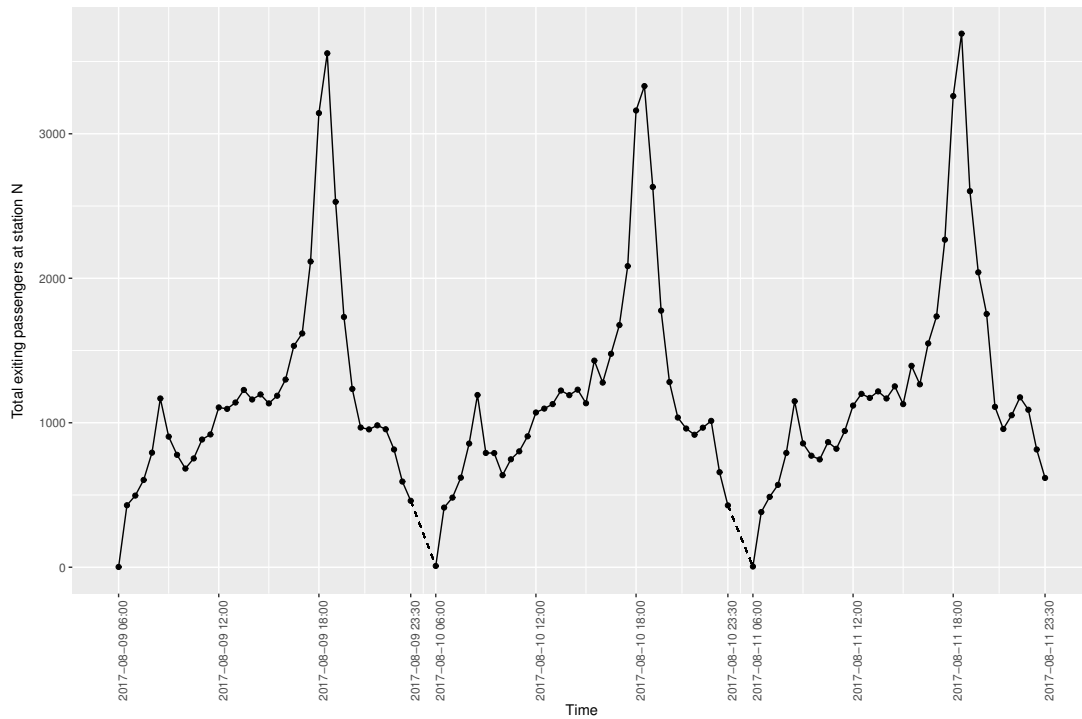


Figure 1: Traffic load in a certain station per half hour

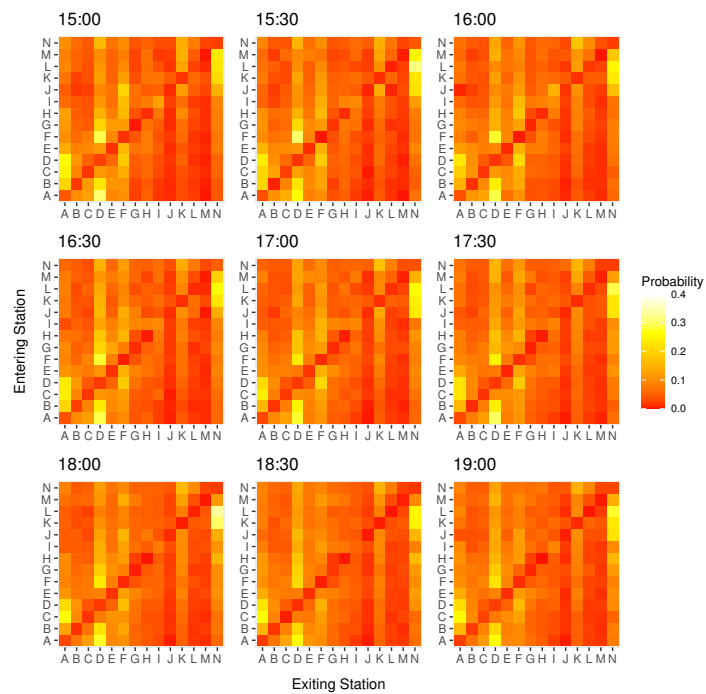


Figure 2: Heat map of some transition probability matrices in a certain line on August 10, 2017.

monitoring of a biodiverse community (Fang and Huang, 2013), periodic orbits embedded in the chaotic attractor (Gao and Jin, 2012), social networks (Chunaev, 2020) and other fields.

About a hundred years ago, the univariate control charts, including Shewhart control chart (Shewhart, 1925), the CUSUM control chart (Page, 1954) and exponentially weighted moving average (EWMA) control chart (Roberts, 1959), were designed to give a signal when an out-of-control (OC) condition came up. With the increasing complexity of the production process, they have been extended to the monitoring of multiple characteristics (Vargas, 2003; Chenouri et al., 2009; Yu et al., 2019; Wang et al., 2021) and even evolved into the network cases (Umakanth and Damodhar, 2013). For directed networks, Woodall et al. (2017) provided an overview of SPC methods developed for social network data, in which the shifts in the communication levels of a network (Azarnoush et al., 2016) and average closeness and betweenness of a network (McCulloh and Carley, 2011) were mainly considered. Besides, Perry (2020) was interested in detecting shifts in the hierarchical tendency of binary digraphs. Time-independence was assumed in these papers, which was usually not match reality as the above examples said, and it has been demonstrated that the conventional control schemes allow a great many false alarms when the independence assumption is violated (Harris and Ross, 1991). Chen et al. (2021) presented a matrix autoregressive model in a bilinear form to achieve the analysis of dynamic networks. The limitation was that it was not able to handle a network with a large amount of nodes, since the computational memory exceeds the machine's capacity easily in this problem.

In the literature, there has been some discussion on the process monitoring of serially correlated data. Residual control charts, that detected the one-step forecast errors, were commonly used on this topic (e.g., Apley and Shi (1999); Schmid and Schöne (1997); Loredó et al. (2002); Li and Tsung (2009)). However, their performance was sensitive to the assumed parametric time series models that usually were invalid in practice. Then some nonparametric algorithms were proposed to monitor those dynamic data with very undemanding requirements, including dynamic screening system (DySS) method (Qiu and Xiang, 2014; Li and Qiu, 2016) and top- $r$  control chart (Yu et al., 2021). The former made use of kernel functions, while the latter mainly detected the shifts of the quasi maximum likelihood estimator (QMLE). Both computationally slow diagnostic procedures had many tuning parameters and would break the robustness of detection easily. To overcome this difficulty, the concept of spring length, which was first discussed in Chatterjee and Qiu (2009),

was well developed in the control algorithms. See, for instance, Li and Qiu (2020), Qiu et al. (2020), Xue and Qiu (2021), and so on. Though its advantage, which was that the only correlation between adjacent points was assumed, was significant, it could only be used in the univariate case. In conclusion, the scalability of these methods will certainly bring new opportunities for research into approaches to model-free monitoring algorithms in network data.

Our paper concentrates on developing a robust and sensitive control scheme to monitor the doubly correlated directed network. The directed network is modeled by transition matrix and the transition probability matrix is regarded as the detection objection. The advantages are reflected in two aspects: weakening the serial correlation and standardizing data. Firstly, there is only one type of serial correlation in the transition probability matrix, that can improve the robustness of control schemes compared with monitoring the transfer matrix directly. Secondly, the sum of each row is one and every element value is between zero and one in a transition probability matrix. Then we can apply the multivariate CUSUM method to each row of data and use a weighted sum of CUSUM statistic to create a new control chart because of their same measurement units. The total number of transitions serves as a weighting function to display the importance of each point in the network. Significantly, we extend the spring-length-based method to the multivariate case to solve the unstable performance of the algorithm that arises from the serial correlation. Compared with conventional control charts, this approach has weaker assumptions and can be applied in practice more easily. In particular, the novel way only assumes that the process observation is associated with nearby points without any parametric time series models. In brief, it is a new insight into constructing a control chart to monitor the above problem.

The remainder of this paper is organized as follows. In the next section, we develop the spring-length-based method to deal with the serially correlated problem in the multivariate case. Section 3 evaluates the performance of the proposed chart in comparison with the advanced CUSUM and EWMA control charts. And a new CUSUM control chart based on the weighted sum of the above uncorrelated statistic is proposed to monitor the transition probability matrix. Furthermore, numerical simulation studies are conducted and performance comparisons are made in Section 3. In Section 4, we introduce a step-by-step illustration of the proposed algorithm and illustrate the superiority of our design using the example of traffic network monitoring. Several remarks conclude the paper and further studies are proposed in Section 5.

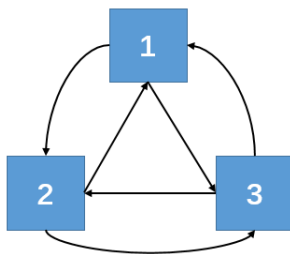


Figure 3: Fully transitive tournament with three vertices

## 2 Methodologies

As Kilduff and Tsai (2003) said, monitoring the relationship between the reciprocal and transitive tendencies in a directed network was a simple technology to assess its shift. To achieve it, the numbers of the transition in the network are digitally represented as a matrix in Section 2.1. Then a de-correlation way in the vector is proposed and used in each row of a serially correlated matrix in Section 2.2. Section 2.3 illustrates a new CUSUM statistic based on the above de-correlation method in the multivariate case. Finally, we design a weighted CUSUM control algorithm to detect the mean shift of the digraph in Section 2.4.

### 2.1 Digital representation of digraph

In a complex directed network, there could be a transitive relationship between any two nodes, for example, see Figure 3.  $n_{ij}^{(t)}$  denotes the total numbers flowing from node  $i$  to node  $j$  at time  $t$ . Then  $n_{ij}^{(t)}$  equal to zero indicates no edge flows from node  $i$  to node  $j$  at time  $t$ . In this setting, Figure 3 suggests a fully transitive tournament with three nodes and it contains all six possible ways to define a transitive flow among the three nodes in Perry (2020).

Assume that we have  $K$  nodes in one digraph, then we can observe a transitive relationship at time  $t$  as follows:

$$\mathcal{N}^{(t)} = \begin{pmatrix} n_{11}^{(t)} & n_{12}^{(t)} & \cdots & n_{1K}^{(t)} \\ n_{21}^{(t)} & n_{22}^{(t)} & \cdots & n_{2K}^{(t)} \\ \cdots & \cdots & \ddots & \cdots \\ n_{K1}^{(t)} & n_{K2}^{(t)} & \cdots & n_{KK}^{(t)} \end{pmatrix}.$$

We call  $\mathcal{N}^{(t)}$  transition matrix that can describe a transitive network well.

As mentioned above,  $\mathcal{N}^{(t)}$  usually is doubly corrected, especially in a complex transportation network. In particular, the total numbers that flow out of the node and the transition probability both are serially correlated. Thus a direct analysis on the  $\mathcal{N}^{(t)}$  may not perform robustly. Furthermore, the scale of the  $n_{ij}^{(t)}$ s ( $i = 1, 2, \dots, K, j = 1, 2, \dots, K$ ) is various, that reflect the importance of each nodes. For instance, the value of  $n_{ij}^{(t)}$  is very large when the nodes  $i$  and  $j$  are active in the network, and is small otherwise. To facilitate the following modeling, the transition probability matrix is applied as our measure of transitive relationship here:

$$\mathcal{P}^{(t)} = \begin{pmatrix} p_{11}^{(t)} & p_{12}^{(t)} & \cdots & p_{1K}^{(t)} \\ p_{21}^{(t)} & p_{22}^{(t)} & \cdots & p_{2K}^{(t)} \\ \cdots & \cdots & \ddots & \cdots \\ p_{K1}^{(t)} & p_{K2}^{(t)} & \cdots & p_{KK}^{(t)} \end{pmatrix},$$

where  $p_{ij}^{(t)} = \frac{n_{ij}^{(t)}}{n_i^{(t)}}$  and  $n_i^{(t)} = \sum_{j=1}^K n_{ij}^{(t)}$ . Then we have  $\sum_{j=1}^K p_{ij}^{(t)} = 1$  ( $i = 1, 2, \dots, K$ ). Thus, the  $i$ -th row data of  $\mathcal{P}^{(t)}$ , that is denoted as  $\mathcal{P}_i^{(t)} = (p_{i1}^{(t)}, p_{i2}^{(t)}, \dots, p_{iK}^{(t)})^T$ , is standardized.

## 2.2 De-correlation approach in the multivariate variables

Recall that  $\boldsymbol{\mu}_i$  and  $\Sigma_i$  are the mean vector and covariance matrix of the  $i$ -th row data of the above transition probability matrix respectively, where any shift in  $\boldsymbol{\mu}_i$  shows the change of the transfer relationship in the network. For example, the shift in the station to station relationship in the metro network reminds operators to make a schedule adjustment in time. Then the problem is equivalent to hypotheses testing:

$$H_0 : \boldsymbol{\mu}_i = \boldsymbol{\mu}_{0,i} \quad \text{V.S.} \quad H_1 : \boldsymbol{\mu}_i = \boldsymbol{\mu}_{1,i}, \quad (1)$$

where  $\boldsymbol{\mu}_{0,i}$  and  $\boldsymbol{\mu}_{1,i}$  are the in-control mean vector and the expected out-of-control mean vector, respectively, and  $\boldsymbol{\mu}_{0,i} \neq \boldsymbol{\mu}_{1,i}$ . Then we common use the traditional multivariate CUSUM control chart based on the independence and normality assumptions to handle it as follows:

$$\begin{aligned} C_{i,t}^+ &= \max(0, C_{i,t-1}^+ + e_{i,t} - k_i) \\ C_{i,t}^- &= \min(0, C_{i,t-1}^- + e_{i,t} + k_i) \end{aligned}, \quad (2)$$

where  $e_{i,t} = (\mathcal{P}_i^{(t)} - \boldsymbol{\mu}_{0,i})^T (\boldsymbol{\Sigma}_i)^{-1} (\boldsymbol{\mu}_{1,i} - \boldsymbol{\mu}_{0,i})$ ,  $k_i = \frac{1}{2} (\boldsymbol{\mu}_{1,i} - \boldsymbol{\mu}_{0,i})^T (\boldsymbol{\Sigma}_i)^{-1} (\boldsymbol{\mu}_{1,i} - \boldsymbol{\mu}_{0,i})$  and  $C_{i,0}^+ = C_{i,0}^+ = 0$ .

As described above, the serial correlation of the  $e_{i,t}$  necessitate a de-correlate process before a control chart is used. Similar with Qiu et al. (2020), we can assume that the observations are covariance stationary and the only two points with a time interval less than  $B$  are serially correlated, where  $B > 0$  is an integer. More specifically, the autocorrelation coefficient  $\gamma_i(q) = \text{cov}(\mathcal{P}_i^{(t)}, \mathcal{P}_i^{(t+q)})$  is a proper measure of the correlation. In practice,  $\gamma_i(q)$  usually decreases with time interval  $q$  because that data is time-sensitive and observations closer to the current point have greater impact. Thus there exists a proper value of  $B$  such that  $\gamma_i(q) = 0$  when  $q > B$ . Furthermore,  $\gamma_i(q)$  can be estimated by

$$\hat{\gamma}_i(q) = \frac{1}{m-q} \sum_{t=-m+1}^{-q} (\mathcal{P}_i^{(t)} - \boldsymbol{\mu}_{0,i})^T (\mathcal{P}_i^{(t+q)} - \boldsymbol{\mu}_{0,i}), \quad (3)$$

where  $\mathcal{P}_i^{(-m+1)}, \mathcal{P}_i^{(-m+2)}, \dots, \mathcal{P}_i^{(0)}$  are IC data and  $m \gg B$ .

According to the Cholesky decomposition of the covariance matrices, we propose the  $t$ -th asymptotically uncorrelated and standardized statistic as

$$\tilde{e}_{i,t} = (\mathcal{P}_i^{(t)} - \boldsymbol{\mu}_{0,i} - \hat{\boldsymbol{\sigma}}_i^T \hat{\Gamma}_i^{-1} \mathbf{e}_i^*)^T \tilde{\boldsymbol{\Sigma}}_i^{-1} (\boldsymbol{\mu}_{1,i} - \boldsymbol{\mu}_{0,i}), \quad (4)$$

where

- $$\tilde{\boldsymbol{\Gamma}}_i = \begin{pmatrix} \hat{\gamma}_i(0) & \cdots & \hat{\gamma}_i(B) \\ \hat{\gamma}_i(1) & \cdots & \hat{\gamma}_i(B-1) \\ \cdots & \ddots & \cdots \\ \hat{\gamma}_i(B) & \cdots & \hat{\gamma}_i(0) \end{pmatrix} = \begin{pmatrix} \hat{\Gamma}_i & \hat{\boldsymbol{\sigma}}_i \\ \hat{\boldsymbol{\sigma}}_i^T & \hat{\gamma}_i(0) \end{pmatrix}.$$

- $\mathbf{e}_i^* = (\mathcal{P}_i^{(t-B)} - \boldsymbol{\mu}_{0,i}, \dots, \mathcal{P}_i^{(t-1)} - \boldsymbol{\mu}_{0,i})$ ,
- $\tilde{\boldsymbol{\Sigma}}_i = (1 - \hat{\boldsymbol{\sigma}}_i^T \hat{\Gamma}_i^{-1} \hat{\boldsymbol{\sigma}}_i) \boldsymbol{\Sigma}_i$ .

The estimation of parameter  $B$  will be discussed in the next subsection.

### 2.3 The new CUSUM statistic for serially correlated vectors

In this subsection, we firstly introduce the spring-length-based method to estimate the parameter  $B$  and then give an improved CUSUM statistic to monitor the row data of the transition probability matrix.

As Qiu et al. (2020) suggested, the spring-length-based method is a proper way to estimate the parameter  $B$ . The spring length was defined as the time length between the current time point and the previous time point when a CUSUM applied to the original process observations is reset to zero (Chatterjee and Qiu, 2009). It indicated that the past observations beyond the spring length of the current time could be ignored since no more useful information would be provided by them. It inspires us that the parameter  $B$  is reset to zero when the CUSUM statistic is equal to zero. In detail, the value of  $B$  can be updated by adding one to the original value when the lag time between the present and the past is within the spring length, zero otherwise. It noticed that the maximum value of  $B$ , denoted as  $B_{max}$ , needs to be pre-specified. On the one hand, though the value of  $B$  should be chosen as large as possible, the estimation of  $\gamma(B)$  is more and more unreliable as  $B$  gets bigger and bigger, especially in the initial period of process monitoring. On the other hand, storing too many past observations is a big challenge for a machine. Of course, the proper value of  $B_{max}$  is often application-specific. For example, the urban metro transportation system only keeps an eye on the last two hours as the expert advice. Above all, we raise an advanced CUSUM statistic to describe the shift in a serially correlated vector:

(1) In the case when  $t = 1$ , the conventional CUSUM statistic is used as

$$\begin{aligned}\tilde{C}_{i,1}^+ &= \max \left( 0, (\mathcal{P}_i^{(t)} - \boldsymbol{\mu}_{0,i})^T (\Sigma_i)^{-1} (\boldsymbol{\mu}_{1,i} - \boldsymbol{\mu}_{0,i}) - \frac{1}{2} (\boldsymbol{\mu}_{1,i} - \boldsymbol{\mu}_{0,i})^T (\Sigma_i)^{-1} (\boldsymbol{\mu}_{1,i} - \boldsymbol{\mu}_{0,i}) \right), \\ \tilde{C}_{i,1}^- &= \min \left( 0, (\mathcal{P}_i^{(t)} - \boldsymbol{\mu}_{0,i})^T (\Sigma_i)^{-1} (\boldsymbol{\mu}_{1,i} - \boldsymbol{\mu}_{0,i}) + \frac{1}{2} (\boldsymbol{\mu}_{1,i} - \boldsymbol{\mu}_{0,i})^T (\Sigma_i)^{-1} (\boldsymbol{\mu}_{1,i} - \boldsymbol{\mu}_{0,i}) \right).\end{aligned}\quad (5)$$

And two-sided control statistic is defined as  $\tilde{C}_{i,1} = \max(\tilde{C}_{i,1}^+, -\tilde{C}_{i,1}^-)$ . Also define the order of correlation at time  $t = 1$  as  $B_{i,1} = 1$  if  $C_{i,1} > 0$  and 0 otherwise.

(2) In the case when  $t \geq 2$ , we consider the following two cases:

- If  $B_{i,t-1} = 0$ , calculate  $C_{i,t}$  and  $B_{i,t}$  in the same way as that in the case when  $t = 1$  discussed above.

- If  $B_{i,t-1} > 0$ , the de-correlation approach in Equation (4) is used here. Let

$$\tilde{\Gamma}_{i,t} = \begin{pmatrix} \hat{\gamma}_i(0) & \cdots & \hat{\gamma}_i(B_{i,t-1}) \\ \hat{\gamma}_i(1) & \cdots & \hat{\gamma}_i(B_{i,t-1} - 1) \\ \cdots & \ddots & \cdots \\ \hat{\gamma}_i(B_{i,t-1}) & \cdots & \hat{\gamma}_i(0) \end{pmatrix} = \begin{pmatrix} \hat{\Gamma}_{i,t-1} & \hat{\boldsymbol{\sigma}}_{i,t-1} \\ \hat{\boldsymbol{\sigma}}_{i,t-1}^T & \hat{\gamma}_i(0) \end{pmatrix}.$$

Then the new CUSUM statistic are defined as

$$\begin{aligned} \tilde{C}_{i,t}^+ &= \max\left(0, \tilde{C}_{i,t-1}^+ + \tilde{e}_{i,t} - k_i\right), \\ \tilde{C}_{i,t}^- &= \min\left(0, \tilde{C}_{i,t-1}^- + \tilde{e}_{i,t} + k_i\right), \end{aligned} \tag{6}$$

where  $\tilde{e}_{i,t} = (\mathcal{P}_i^{(t)} - \boldsymbol{\mu}_{0,i} - \hat{\boldsymbol{\sigma}}_{i,t-1}^T \hat{\Gamma}_{i,t-1}^{-1} \mathbf{e}_{i,t-1}^*)^T \tilde{\Sigma}_{i,t}^{-1} (\boldsymbol{\mu}_{1,i} - \boldsymbol{\mu}_{0,i})$ ,  $\mathbf{e}_{i,t-1}^* = (\mathcal{P}_i^{(t-B_{i,t-1})} - \boldsymbol{\mu}_{0,i}, \dots, \mathcal{P}_i^{(t-1)} - \boldsymbol{\mu}_{0,i})$ , and  $\tilde{\Sigma}_{i,t} = (1 - \hat{\boldsymbol{\sigma}}_{i,t-1}^T \hat{\Gamma}_{i,t-1}^{-1} \hat{\boldsymbol{\sigma}}_{i,t-1}) \Sigma_i$ .

$$\text{Similarly, } \tilde{C}_{i,t} = \max\left(\tilde{C}_{i,t}^+, -\tilde{C}_{i,t}^-\right) \text{ and } B_{i,t} = \begin{cases} \max(B_{max}, B_{i,t-1} + 1), & \tilde{C}_{i,t} > 0, \\ 0, & \tilde{C}_{i,t} = 0. \end{cases}$$

## 2.4 The weighted CUSUM control algorithm for whole network detection

We design an adaptive weighted CUSUM control algorithm to achieve the detection of the whole transition probability matrix here.

Though we have achieved the row data detection, we can not simply apply the other traditional control charts (e.g., top- $r$  control scheme (Mei, 2010)) to monitor the network in consideration of the endogenous structure of the network. In this setting, the one benefit of the transition probability matrix detection, in which the sum of each row is one, is there. We can regard each row of data as asymptotically independent observations by excluding the effect of the data size in each node. But obviously, the importance of each node is different. The shift that happened in a more active node should be paid more attention to. Thus, we propose an adaptive weighted-sum statistic to detect the whole directed network. At the time  $t$ , the weighting function and the adaptive weighted-sum statistic are defined as

$$w_i^{(t)} = \frac{n_i^{(t)}}{\sum_{i=1}^K n_i^{(t)}}, \tag{7}$$

and

$$\tilde{C}_t = \sum_{i=1}^K w_i^{(t)} \tilde{C}_{i,t}. \quad (8)$$

The CUSUM chart defined in Equations (8) gives a signal of mean shift when

$$\tilde{C}_t > h, \quad (9)$$

where  $h > 0$  is the control limit.

In a word, the adaptive weighted CUSUM control algorithm is shown in Algorithm 1.

### 3 Simulation Performance

In this section, the numerical performance of the proposed methodology is demonstrated, including the singly and doubly serial correlation cases, respectively, and the case of correlated row data.

The average and standard deviation of run length, which is defined as the sampling until an out-of-control signal emerges, are commonly used to evaluate the control charts' performance. Concretely, we prefer a long IC average run length ( $ARL_0$ ) and a short OC average run length ( $ARL_1$ ), while a short standard deviation of run length (SDRL) is desired. The following results are calculated from 10000 replicated simulations.

Besides the proposed control scheme in Algorithm 1, denoted as WSCUSUM, the following four types of control charts are considered for comparison purposes:

- (1) The conventional top-1 CUSUM chart proposed by Mei (2010), denoted as TCUSUM, has the charting statistic defined in Equation (2). The chart gives a signal when the statistic

$$\max_{i=1,2,\dots,K} \max(C_{i,t}^+, -C_{i,t}^-) \text{ exceeds the control limit.}$$

- (2) The de-correlated conventional top-1 CUSUM control chart, denoted as DTCUSUM, has the charting statistic defined in Equation (6). The chart gives a signal when the statistic

$$\max_{i=1,2,\dots,K} \max(\tilde{C}_{i,t}^+, -\tilde{C}_{i,t}^-) \text{ exceeds the control limit.}$$

- (3) Similar with the above de-correlated conventional top-1 CUSUM control chart, the control chart, denoted as DTCUSUM-n, is designed for the detection of  $\mathcal{N}^{(t)}$  instead of  $\mathcal{P}^{(t)}$ .

---

**Algorithm 1** The weighted CUSUM control algorithm for serially correlated directed network detection

---

**Input:**

- IC data  $\mathcal{P}^{(-m+1)}, \mathcal{P}^{(-m+2)}, \dots, \mathcal{P}^{(0)}$ ;
- IC and expected OC mean vector of each row data  $\boldsymbol{\mu}_{0,i}$  and  $\boldsymbol{\mu}_{1,i}$  ( $i = 1, 2, \dots, K$ ) respectively;
- The covariance matrix of each row data  $\Sigma_i$  ( $i = 1, 2, \dots, K$ );
- The control limit  $h$ ;
- $\tilde{C}_0 = 0$  and  $B_0 = 0$ .

```

1: for  $i = 1, 2, \dots, K$  do
2:   Compute  $k_i = \frac{1}{2}(\boldsymbol{\mu}_{1,i} - \boldsymbol{\mu}_{0,i})^T(\boldsymbol{\Sigma}_i)^{-1}(\boldsymbol{\mu}_{1,i} - \boldsymbol{\mu}_{0,i})$ ;
3: end for
4: for  $t = 1, 2, \dots$  do
5:   Observe  $\mathcal{N}^{(t)}$ ;
6:   Compute  $\mathcal{P}^{(t)}$ ;
7:   if  $B_{t-1} = 0$  then
8:     for  $i = 1, 2, \dots$  do
9:       Compute  $\tilde{e}_{i,t} = (\mathcal{P}_i^{(t)} - \boldsymbol{\mu}_{0,i})^T(\boldsymbol{\Sigma}_i)^{-1}(\boldsymbol{\mu}_{1,i} - \boldsymbol{\mu}_{0,i})$ ;
10:    end for
11:   else
12:     for  $i = 1, 2, \dots$  do
13:       Compute

```

$$\tilde{\Gamma}_{i,t} = \begin{pmatrix} \hat{\gamma}_i(0) & \cdots & \hat{\gamma}_i(B_{t-1}) \\ \hat{\gamma}_i(1) & \cdots & \hat{\gamma}_i(B_{t-1} - 1) \\ \cdots & \ddots & \cdots \\ \hat{\gamma}_i(B_{t-1}) & \cdots & \hat{\gamma}_i(0) \end{pmatrix} = \begin{pmatrix} \hat{\Gamma}_{i,t-1} & \hat{\boldsymbol{\sigma}}_{i,t-1} \\ \hat{\boldsymbol{\sigma}}_{i,t-1}^T & \hat{\gamma}_i(0) \end{pmatrix};$$

```

14:       Compute  $\tilde{\Sigma}_{i,t} = (1 - \hat{\boldsymbol{\sigma}}_{i,t-1}^T \hat{\Gamma}_{i,t-1}^{-1} \hat{\boldsymbol{\sigma}}_{i,t-1})\boldsymbol{\Sigma}_i$ ;
15:       Compute  $\tilde{e}_{i,t} = (\mathcal{P}_i^{(t)} - \boldsymbol{\mu}_{0,i} - \hat{\boldsymbol{\sigma}}_{i,t-1}^T \hat{\Gamma}_{i,t-1}^{-1} \mathbf{e}_{i,t-1}^*)^T \tilde{\Sigma}_{i,t}^{-1}(\boldsymbol{\mu}_{1,i} - \boldsymbol{\mu}_{0,i})$ , where  $\mathbf{e}_{i,t-1}^* =$ 
 $(\mathcal{P}_i^{(t-B_{t-1})} - \boldsymbol{\mu}_{0,i}, \dots, \mathcal{P}_i^{(t-1)} - \boldsymbol{\mu}_{0,i})$ ;
16:     end for
17:   end if
18:   Compute  $\tilde{C}_{i,t}^+ = \max(0, \tilde{C}_{i,t}^+ + \tilde{e}_{i,t} - k_i)$ ,  $\tilde{C}_{i,t}^- = \min(0, \tilde{C}_{i,t}^- + \tilde{e}_{i,t} + k_i)$  and  $\tilde{C}_{i,t} =$ 
 $\max(\tilde{C}_{i,t}^+, -\tilde{C}_{i,t}^-)$ ;
19:   Compute  $\tilde{C}_t = \sum_{i=1}^K w_i^{(t)} \max(\tilde{C}_{i,t}^+, -\tilde{C}_{i,t}^-)$ , where  $w_i^{(t)} = \frac{n_i^{(t)}}{\sum_{i=1}^K n_i^{(t)}}$ ;
20:   Compute  $B_t = \begin{cases} \max(B_{max}, B_{t-1} + 1), & \tilde{C}_t > 0, \\ 0, & \tilde{C}_t = 0. \end{cases}$ 
21: end for

```

**Output:** An early warning when  $\tilde{C}_t > h$ .

---

(4) The EWMA control chart with applications to social network monitoring proposed by Perry (2020), denoted as NEWMA, has the charting statistic as

$$\begin{aligned} G_{i,0} &= 0, \\ G_{i,t} &= (1 - \lambda)G_{i,t-1} + \lambda U_{i,t}, \end{aligned} \tag{10}$$

where  $U_{i,t} = \left( \sum_{j=1}^K \frac{p_{ij}^{(t)}}{\mu_{0,ij} \times n_i^{(t)}} - K \right) / \sigma_i^*$ , where  $\mu_{0,ij}$  is the  $j$ -th element of  $\boldsymbol{\mu}_{0,i}$ , and  $\sigma_i^{*2} = \frac{1}{n_i^{(t)}} \left( \sum_{j=1}^K \frac{1 - \mu_{0,ij}}{\mu_{0,ij}} - K(K - 1) \right)$ . The upper and lower control limits are given by  $UCL_t/LCL_t = \pm L \sqrt{\frac{\lambda}{2 - \lambda} [1 - (1 - \lambda)^{2t}]}$ , where  $L$  is a parameter that can be estimated from the simulation studies in a given  $ARL_0$  setting. The chart gives a signal when the any statistic  $G_{i,t}$  is larger than  $UCL_t$  or less than  $LCL_t$ . The weighting parameter  $\lambda$  is fixed at 0.1.

Without loss of generality, the IC mean matrix of  $\mathcal{P}^{(t)}$  is  $\begin{pmatrix} 0.45 & 0.55 \\ 0.95 & 0.05 \end{pmatrix}$ , that demonstrates the two cases of uniform and large transition probability between two nodes, and expected OC mean matrix of  $\mathcal{P}^{(t)}$  is  $\begin{pmatrix} 0.5 & 0.5 \\ 0.5 & 0.5 \end{pmatrix}$ . According to the suggestion of Li and Qiu (2020), the IC dataset of size  $m = 1000$  is obtained to estimate the IC mean vector, covariance matrix and correlation coefficient. In the above settings, we design three scenarios, that is  $(n_1^{(0)}, n_2^{(0)}) = (100, 100)$ ,  $(n_1^{(0)}, n_2^{(0)}) = (100, 500)$ , and  $(n_1^{(0)}, n_2^{(0)}) = (100, 30)$ , with  $ARL_0 \approx 200$ . These cases are studied in the various AR(1) models and we choose  $B_{max} = 4$  in this paper.

### 3.1 The performance in a singly and doubly serial correlation case

In this subsection, denote the true mean matrix of  $\mathcal{P}^{(t)}$  as  $\boldsymbol{\mu} = \begin{pmatrix} \mu_{11} & 1 - \mu_{11} \\ 1 - \mu_{22} & \mu_{22} \end{pmatrix}$ . We assume the only one of three, that is  $\mathcal{P}^{(t)}$ ,  $\mathcal{N}^{(t)}$  and  $(n_1^{(t)}, n_2^{(t)})$ , is serially correlated:

- Condition I: Observations  $\mathcal{N}^{(t)}$  ( $t = 1, 2, \dots$ ) follow the AR(1) model:

$$\begin{aligned} \begin{pmatrix} n_{11}^{(t)} \\ n_{12}^{(t)} \end{pmatrix} &= \max \left( \begin{pmatrix} 0 \\ 0 \end{pmatrix}, \left[ 0.5 \begin{pmatrix} n_{11}^{(t-1)} \\ n_{12}^{(t-1)} \end{pmatrix} + 0.5\epsilon_1 \right] \right), \\ \begin{pmatrix} n_{21}^{(t)} \\ n_{22}^{(t)} \end{pmatrix} &= \max \left( \begin{pmatrix} 0 \\ 0 \end{pmatrix}, \left[ 0.9 \begin{pmatrix} n_{21}^{(t-1)} \\ n_{22}^{(t-1)} \end{pmatrix} + 0.1\epsilon_2 \right] \right), \end{aligned} \quad (11)$$

where  $\epsilon_1^{(t)}$  and  $\epsilon_2^{(t)}$  ( $t = 1, 2, \dots$ ) are independent identically distributed (i.i.d.) with the distribution  $N((\mu_{11}n_1, n_1 - \mu_{11}n_1)^T, \text{diag}(16, 16))$  and  $N((n_2 - \mu_{22}n_2, \mu_{22}n_2)^T, \text{diag}(16, 16))$  respectively, and  $[a]$  represents the largest integer not exceeding  $a$ .

- Condition II: Transition probability  $\mathcal{P}^{(t)}$  ( $t = 1, 2, \dots$ ) follow the AR(1) model:

$$\begin{aligned} p_{11}^{(t)} &= \min \left( 1, \left( 0.5p_{11}^{(t-1)} + 0.5\dot{\epsilon}_1^{(t)} \right) \vee 0 \right), \\ p_{22}^{(t)} &= \min \left( 1, \left( 0.9p_{22}^{(t-1)} + 0.1\dot{\epsilon}_2^{(t)} \right) \vee 0 \right), \end{aligned} \quad (12)$$

where  $a \vee b = \begin{cases} a, a \geq b, \\ b, a < b, \end{cases}$ ,  $\dot{\epsilon}_1^{(t)}$  and  $\dot{\epsilon}_2^{(t)}$  ( $t = 1, 2, \dots$ ) are i.i.d. with the distribution

$N(p_{11}^{(t-1)}, 0.0001)$  and  $N(p_{22}^{(t-1)}, 0.0001)$  respectively. Then  $p_{12}^{(t)} = 1 - p_{11}^{(t)}$  and  $p_{21}^{(t)} = 1 - p_{22}^{(t)}$ .

And let  $n_{ij}^{(t)} \sim \text{multinomial}(n_i^{(t)}; p_{ij})$  ( $i, j = 1, 2$ ).

- Condition III: Total number of transition  $(n_1^{(t)}, n_2^{(t)})$  follow the AR(1) model:

$$\begin{aligned} n_1^{(t)} &= \max(0, [0.5n_1^{(t-1)} + 0.5\ddot{\epsilon}_1^{(t)}]), \\ n_2^{(t)} &= \max(0, [0.9n_2^{(t-1)} + 0.1\ddot{\epsilon}_2^{(t)}]), \end{aligned} \quad (13)$$

where  $\ddot{\epsilon}_1^{(t)}$  and  $\ddot{\epsilon}_2^{(t)}$  ( $t = 1, 2, \dots$ ) are i.i.d. with the distribution  $N(n_1^{(t-1)}, 100)$  and  $N(n_2^{(t-1)}, 100)$  respectively. Then let  $n_{ij}^{(t)} \sim \text{multinomial}(n_i^{(t)}; p_{ij})$  ( $i, j = 1, 2$ ).

Table 1-3 only show that the shift only happens in  $(\mu_{11}, 1 - \mu_{11})^T$ . More extensive results for shifts happens in other cases will be studied in Section 3.3.

Firstly, the feasibility of transition probability matrix detection is verified by the simulation results, since SDRs of the DTCUSUM-n control chart, which monitors the transition matrix only,

usually are bigger than the other four control schemes, which monitor transition probability matrix, whether the shifts occur in the transition number, total number, or transition probability. From Table 1, we can conclude that:

- Compared with TCUSUM, DTCUSUM and NEWMA control charts, our proposed method overcome the non-monotonically decreasing property of the ARLs with the increasing of the shift, especially in the case of small shifts;
- Compared with TCUSUM and NEWMA control charts, our control scheme has smaller SDRLs in the small shift. Moreover, the SDRLs in the TCUSUM and NEWMA are much larger than the ARLs in them, which means that these two control charts are extremely unreliable when they detect the small shifts. On the contrary, the WSCUSUM control chart is robust in various cases based on the fact that its SDRLs are always less than the corresponding ARLs;
- Our control scheme has a most sensitive performance in monitoring the small shifts, especially when the transition numbers are small and  $|\mu_{11} - \mu_{0,11}| \leq 0.05$ , since its ARLs are smallest;
- The increasing of transition numbers can fix our slow warning during large shifts.

Similar results also can be found in Table 2 and Table 3.

When considering the different serial correlation cases, the robustness of the WSCUSUM control chart is most prominently displayed in two ways: (i) The  $ARL_1$  always becomes smaller with an increasing mean shift and initial total number of transition; (ii) The SDRLs are always smaller than the corresponding ARLs. Furthermore, compared with the results in Table 1 and Table 3, the WSCUSUM control chart performs best in Condition II, that is the transition probability matrix is serially correlated, with the smaller ARLs and SDRLs as expected.

Overall, the WCUSUM has unique advantages in terms of robustness. Though it is not the most sensitive in some cases, its performance in ARLs is acceptable.

### 3.2 The performance in a doubly serial correlation case

In this subsection, we study the control schemes' performance in case of doubly serial correlation, that is the total number and probability of transition are both serially correlated. The following

Table 1: The ARL performance of different control charts in Condition I (the corresponding SDRIs are shown in parentheses).

$\mu_{11}$	$(n_1, n_2) = (100, 100)$					$(n_1, n_2) = (100, 500)$					$(n_1, n_2) = (100, 30)$					
	WCSUM	TCUSUM	DTCUSUM	NEWMA	NEWMA	WCSUM	TCUSUM	DTCUSUM	NEWMA	NEWMA	WCSUM	TCUSUM	DTCUSUM	DTCUSUM	NEWMA	NEWMA
0.45	200.21 (164.72)	200.24 (163.38)	198.27 (580.09)	200.99 (223.86)	200.68 (214.14)	200.53 (163.46)	200.68 (214.14)	199.93 (168.24)	199.53 (581.73)	200.46 (299.85)	199.68 (176.31)	200.01 (213.65)	199.23 (172.78)	199.02 (581.21)	200.94 (193.34)	200.94 (193.34)
0.449	200.01 (162.80)	203.51 (175.45)	203.67 (587.49)	198.48 (221.34)	204.03 (219.85)	196.00 (189.35)	204.03 (219.85)	210.50 (171.76)	400.74 (788.70)	191.62 (289.64)	199.63 (177.80)	199.10 (214.59)	199.34 (175.18)	199.53 (580.35)	200.38 (195.98)	200.38 (195.98)
0.448	198.82 (164.92)	195.62 (166.72)	205.17 (589.36)	197.24 (217.06)	197.73 (211.87)	189.44 (153.65)	197.73 (211.87)	199.63 (164.12)	390.54 (780.83)	174.31 (260.97)	196.81 (169.89)	193.88 (208.27)	201.04 (174.80)	189.77 (567.62)	199.62 (191.70)	199.62 (191.70)
0.447	162.17 (124.99)	179.87 (189.16)	209.93 (596.12)	197.64 (218.12)	181.93 (191.80)	168.41 (133.01)	181.93 (191.80)	168.16 (151.20)	399.53 (787.79)	145.29 (213.13)	194.85 (170.45)	177.90 (186.62)	201.59 (177.30)	187.40 (564.51)	198.21 (192.99)	198.21 (192.99)
0.446	144.99 (108.37)	166.64 (127.94)	203.86 (587.76)	197.76 (222.07)	169.06 (178.82)	152.89 (117.45)	169.06 (178.82)	152.39 (116.35)	392.83 (782.75)	132.00 (196.78)	184.03 (158.91)	165.91 (177.60)	198.66 (173.65)	200.47 (583.12)	201.75 (195.60)	201.75 (195.60)
0.445	117.87 (81.59)	147.79 (116.68)	198.21 (580.11)	195.36 (216.90)	148.91 (162.52)	128.30 (93.01)	148.91 (162.52)	128.34 (92.33)	400.66 (788.99)	108.62 (159.10)	171.68 (144.23)	147.96 (160.05)	198.44 (180.07)	195.86 (577.09)	200.90 (195.79)	200.90 (195.79)
0.44	55.52 (28.85)	69.39 (28.08)	180.68 (558.09)	200.11 (221.71)	61.81 (77.04)	61.81 (77.04)	70.77 (33.88)	61.53 (33.88)	350.45 (749.71)	40.36 (54.30)	118.25 (76.55)	69.14 (75.90)	198.08 (173.92)	180.77 (558.07)	201.17 (196.15)	201.17 (196.15)
0.435	34.71 (14.28)	33.69 (14.27)	140.12 (496.73)	201.48 (226.42)	37.95 (36.23)	37.95 (36.23)	37.74 (17.20)	37.74 (17.20)	316.17 (720.83)	19.55 (23.22)	81.89 (39.01)	33.45 (35.58)	173.56 (120.65)	151.06 (514.96)	200.89 (195.72)	200.89 (195.72)
0.43	25.22 (8.96)	18.08 (8.71)	106.10 (436.14)	185.51 (205.48)	18.13 (18.77)	26.65 (10.73)	18.13 (18.77)	26.58 (10.73)	242.82 (645.29)	11.32 (11.60)	65.53 (26.36)	17.79 (18.59)	142.12 (77.52)	109.99 (443.83)	200.21 (197.52)	200.21 (197.52)
0.425	19.84 (6.09)	10.72 (5.87)	77.00 (373.98)	137.39 (143.56)	10.74 (10.73)	20.17 (7.50)	10.74 (10.73)	20.21 (7.46)	193.06 (583.75)	7.81 (7.10)	54.82 (20.07)	10.78 (10.75)	117.82 (54.91)	83.10 (388.45)	202.68 (194.66)	202.68 (194.66)
0.42	16.60 (4.53)	6.98 (4.35)	47.51 (293.70)	74.70 (70.84)	16.19 (6.58)	16.19 (6.58)	16.20 (5.43)	16.20 (5.43)	122.62 (472.91)	6.01 (5.01)	48.01 (16.34)	6.96 (6.57)	100.90 (41.23)	57.93 (325.55)	200.33 (193.59)	200.33 (193.59)
0.415	14.16 (3.43)	5.03 (4.46)	32.82 (243.72)	37.89 (30.12)	13.43 (4.41)	13.43 (4.41)	13.41 (4.01)	13.41 (4.01)	95.20 (419.47)	4.81 (3.68)	42.46 (13.97)	4.92 (4.31)	88.66 (33.23)	42.89 (280.46)	184.60 (179.19)	184.60 (179.19)
0.41	12.66 (2.69)	3.69 (3.08)	20.27 (189.83)	23.53 (15.20)	11.56 (3.06)	11.56 (3.06)	11.54 (3.22)	11.54 (3.22)	64.12 (345.88)	3.93 (2.80)	38.20 (12.48)	3.75 (3.10)	78.46 (26.86)	27.76 (224.71)	125.16 (111.21)	125.16 (111.21)
0.405	11.52 (2.14)	3.02 (2.33)	11.12 (136.75)	16.58 (9.38)	3.05 (2.41)	10.22 (2.68)	3.05 (2.65)	10.21 (2.65)	38.92 (269.39)	3.32 (2.19)	34.80 (11.31)	3.00 (2.32)	70.25 (23.31)	17.19 (174.77)	65.66 (49.15)	65.66 (49.15)
0.4	10.65 (1.83)	2.47 (1.78)	4.85 (82.38)	12.41 (6.29)	2.46 (1.74)	2.46 (1.74)	2.46 (2.46)	2.46 (2.46)	21.23 (196.97)	2.90 (1.81)	31.37 (9.61)	2.47 (1.80)	63.75 (19.52)	9.50 (22.80)	38.79 (22.80)	38.79 (22.80)
0.35	7.08 (0.61)	1.08 (0.29)	1.00 (0.02)	9.96 (4.59)	1.08 (0.29)	4.30 (0.96)	1.08 (0.29)	4.32 (0.99)	1.00 (0.03)	1.23 (0.46)	17.50 (3.95)	1.08 (0.29)	33.70 (6.73)	1.00 (0.02)	6.04 (1.57)	6.04 (1.57)
0.3	5.98 (0.31)	1.00 (0.03)	1.00 (0.00)	2.89 (0.97)	1.00 (0.02)	4.00 (0.00)	1.00 (0.03)	4.00 (0.03)	1.00 (0.00)	1.00 (0.06)	13.52 (3.74)	1.00 (0.02)	24.26 (3.74)	1.00 (0.00)	2.94 (0.71)	2.94 (0.71)
0.25	5.46 (0.50)	1.00 (0.00)	1.00 (0.00)	1.53 (0.55)	1.00 (0.00)	4.00 (0.00)	1.00 (0.00)	4.00 (0.00)	1.00 (0.00)	1.00 (0.00)	11.39 (2.02)	1.00 (0.00)	19.29 (2.52)	1.00 (0.00)	1.92 (0.40)	1.92 (0.40)
0.2	5.02 (0.13)	1.00 (0.00)	1.00 (0.00)	1.03 (0.18)	1.00 (0.00)	4.00 (0.00)	1.00 (0.00)	4.00 (0.00)	1.00 (0.00)	1.00 (0.00)	10.03 (1.65)	1.00 (0.00)	16.31 (1.97)	1.00 (0.00)	1.24 (0.43)	1.24 (0.43)
0.15	5.00 (0.00)	1.00 (0.00)	1.00 (0.00)	1.00 (0.00)	1.00 (0.00)	4.00 (0.00)	1.00 (0.00)	4.00 (0.00)	1.00 (0.00)	1.00 (0.00)	9.13 (1.42)	1.00 (0.00)	14.28 (1.65)	1.00 (0.00)	1.00 (0.06)	1.00 (0.06)
0.1	5.00 (0.00)	1.00 (0.00)	1.00 (0.00)	1.00 (0.00)	1.00 (0.00)	4.00 (0.00)	1.00 (0.00)	4.00 (0.00)	1.00 (0.00)	1.00 (0.00)	8.42 (1.24)	1.00 (0.00)	12.81 (1.42)	1.00 (0.00)	1.00 (0.00)	1.00 (0.00)
0.05	5.00 (0.00)	1.00 (0.00)	1.00 (0.00)	1.00 (0.00)	1.00 (0.00)	4.00 (0.05)	1.00 (0.00)	3.99 (0.11)	1.00 (0.00)	1.00 (0.00)	7.93 (1.13)	1.00 (0.00)	11.73 (1.28)	1.00 (0.00)	1.00 (0.00)	1.00 (0.00)

Table 2: The ARL performance of different control charts in Condition II (the corresponding SDRIs are shown in parentheses).

$\mu_{11}$	$(n_1, n_2) = (100, 100)$					$(n_1, n_2) = (100, 500)$					$(n_1, n_2) = (100, 30)$									
	WCSUM	TCUSUM	DTCUSUM	NEWMA	NEWMA	WCSUM	TCUSUM	DTCUSUM	NEWMA	NEWMA	WCSUM	TCUSUM	DTCUSUM	NEWMA	NEWMA	WCSUM	TCUSUM	DTCUSUM	NEWMA	NEWMA
0.45	200.83 (177.84)	199.49 (192.32)	199.21 (565.91)	200.09 (168.29)	200.11 (206.89)	199.27 (169.25)	199.37 (191.53)	199.82 (168.54)	200.52 (247.76)	200.94 (205.86)	200.41 (170.75)	200.47 (194.65)	200.66 (204.26)	200.01 (195.32)	200.17 (206.43)	200.66 (204.26)	200.47 (194.65)	200.66 (204.26)	200.01 (195.32)	200.17 (206.43)
0.449	188.96 (168.69)	196.70 (190.93)	179.31 (531.33)	191.87 (159.34)	198.37 (198.38)	192.03 (161.05)	243.12 (233.08)	192.74 (161.37)	195.92 (237.55)	199.37 (199.72)	189.62 (155.81)	197.69 (192.44)	190.27 (190.06)	195.30 (194.64)	195.30 (198.51)	190.27 (190.06)	197.69 (192.44)	190.27 (190.06)	195.30 (194.64)	195.30 (198.51)
0.448	186.51 (163.81)	191.40 (183.57)	170.13 (503.02)	179.90 (150.13)	196.85 (199.87)	180.10 (151.58)	233.34 (226.18)	180.56 (152.36)	186.06 (227.08)	196.56 (198.86)	178.51 (148.18)	193.31 (185.81)	176.42 (177.48)	200.74 (193.88)	193.31 (197.67)	176.42 (177.48)	193.31 (185.81)	176.42 (177.48)	200.74 (193.88)	193.31 (197.67)
0.447	184.75 (165.17)	180.79 (175.96)	135.36 (431.95)	165.93 (140.04)	187.57 (191.99)	164.40 (140.15)	221.15 (213.21)	164.94 (141.18)	170.96 (211.30)	188.32 (189.48)	163.52 (135.95)	182.26 (178.83)	160.26 (158.88)	200.64 (194.84)	182.26 (191.17)	160.26 (158.88)	182.26 (178.83)	160.26 (158.88)	200.64 (194.84)	182.26 (191.17)
0.446	179.92 (161.79)	169.53 (162.32)	106.21 (359.55)	146.00 (119.17)	173.53 (175.59)	143.89 (117.10)	205.68 (202.09)	144.07 (117.32)	155.40 (192.35)	172.81 (175.84)	143.86 (113.32)	169.88 (161.93)	140.29 (135.47)	197.74 (190.38)	169.88 (177.85)	140.29 (135.47)	169.88 (161.93)	140.29 (135.47)	197.74 (190.38)	169.88 (177.85)
0.445	164.38 (146.74)	157.14 (151.91)	77.33 (265.48)	129.25 (100.65)	159.74 (163.29)	127.84 (101.88)	194.62 (192.23)	127.85 (100.98)	135.83 (162.52)	161.29 (162.36)	127.77 (100.22)	158.31 (153.24)	124.57 (119.78)	196.99 (183.57)	158.31 (161.69)	124.57 (119.78)	158.31 (153.24)	124.57 (119.78)	196.99 (183.57)	158.31 (161.69)
0.44	92.78 (74.77)	101.29 (95.06)	26.38 (73.78)	73.03 (48.28)	98.84 (96.78)	71.01 (47.29)	117.07 (113.00)	70.90 (47.37)	73.01 (85.31)	99.79 (97.27)	72.28 (46.46)	101.52 (94.86)	69.99 (54.99)	158.42 (120.98)	98.06 (96.36)	69.99 (54.99)	101.52 (94.86)	69.99 (54.99)	158.42 (120.98)	98.06 (96.36)
0.435	54.91 (37.66)	62.76 (57.10)	15.64 (36.85)	48.40 (26.14)	58.59 (55.34)	46.46 (26.06)	70.38 (64.10)	46.45 (25.95)	41.84 (43.67)	58.81 (54.53)	49.16 (36.89)	62.60 (57.14)	46.93 (31.77)	117.39 (70.08)	58.34 (55.57)	46.93 (31.77)	62.60 (57.14)	46.93 (31.77)	117.39 (70.08)	58.34 (55.57)
0.43	36.69 (21.91)	39.76 (33.70)	12.19 (25.37)	35.88 (16.36)	37.14 (31.79)	33.99 (16.25)	43.45 (37.90)	34.05 (16.28)	28.21 (26.75)	37.12 (31.32)	36.89 (16.86)	39.65 (33.60)	35.24 (21.05)	90.13 (43.71)	36.35 (31.82)	35.24 (21.05)	39.65 (33.60)	35.24 (21.05)	90.13 (43.71)	36.35 (31.82)
0.425	27.58 (13.79)	27.31 (23.79)	9.68 (18.32)	28.73 (11.29)	24.94 (20.43)	26.90 (11.30)	28.99 (23.23)	26.95 (11.32)	20.58 (17.70)	25.01 (20.39)	29.69 (11.77)	27.37 (21.83)	28.70 (15.15)	30.93 (30.93)	24.84 (20.41)	28.70 (15.15)	29.69 (11.77)	28.70 (15.15)	30.93 (30.93)	24.84 (20.41)
0.42	21.99 (9.86)	19.79 (14.96)	8.28 (14.36)	23.82 (8.22)	18.35 (14.11)	22.17 (8.23)	21.03 (15.67)	22.16 (8.25)	15.93 (12.38)	18.28 (14.06)	24.77 (8.55)	19.57 (11.73)	24.20 (11.73)	60.97 (22.63)	18.29 (14.43)	24.20 (11.73)	19.57 (11.73)	24.20 (11.73)	60.97 (22.63)	18.29 (14.43)
0.415	18.43 (7.35)	15.30 (10.46)	7.42 (12.05)	20.71 (6.36)	13.93 (10.14)	19.04 (6.52)	16.09 (10.99)	19.04 (6.51)	13.03 (9.49)	14.05 (10.18)	21.72 (6.83)	15.19 (10.33)	21.17 (17.33)	52.58 (10.14)	13.79 (10.14)	21.17 (17.33)	15.19 (10.33)	21.17 (17.33)	52.58 (10.14)	13.79 (10.14)
0.41	15.93 (5.77)	12.36 (7.81)	6.62 (10.04)	18.39 (5.13)	11.25 (7.86)	16.68 (5.18)	12.77 (8.13)	16.64 (5.15)	11.01 (7.69)	11.24 (7.84)	19.23 (5.37)	12.37 (7.87)	18.72 (13.76)	10.91 (7.80)	10.91 (7.80)	18.72 (13.76)	12.37 (7.87)	18.72 (13.76)	10.91 (7.80)	10.91 (7.80)
0.405	14.02 (4.46)	10.13 (5.90)	5.94 (8.41)	16.68 (4.13)	9.04 (6.00)	14.94 (4.26)	10.49 (6.14)	14.95 (4.27)	9.46 (6.38)	9.12 (5.95)	17.43 (4.52)	10.01 (5.83)	16.97 (6.86)	9.00 (6.07)	9.00 (6.07)	16.97 (6.86)	10.01 (5.83)	16.97 (6.86)	9.00 (6.07)	9.00 (6.07)
0.4	12.65 (3.70)	8.53 (4.59)	5.66 (7.67)	15.18 (3.39)	7.61 (4.90)	13.52 (3.54)	8.88 (4.73)	13.53 (3.53)	8.32 (5.36)	7.59 (4.86)	16.03 (3.78)	8.55 (4.59)	15.56 (5.94)	7.52 (4.93)	7.52 (4.93)	15.56 (5.94)	8.55 (4.59)	15.56 (5.94)	7.52 (4.93)	7.52 (4.93)
0.35	7.11 (1.24)	3.43 (2.17)	3.41 (2.17)	9.33 (0.99)	2.48 (1.30)	7.59 (1.18)	3.55 (1.16)	7.61 (1.18)	3.91 (1.66)	2.50 (1.30)	9.81 (1.31)	3.41 (1.12)	9.57 (2.64)	2.47 (1.30)	2.47 (1.30)	9.57 (2.64)	3.41 (1.12)	9.57 (2.64)	2.47 (1.30)	2.47 (1.30)
0.3	5.05 (1.37)	2.23 (0.52)	3.02 (0.42)	7.59 (0.55)	1.42 (0.60)	5.78 (0.65)	2.31 (0.55)	5.79 (0.64)	3.09 (0.64)	1.41 (0.59)	7.94 (0.78)	2.23 (0.53)	7.76 (1.73)	1.41 (0.59)	1.41 (0.59)	7.76 (1.73)	2.23 (0.53)	7.76 (1.73)	1.41 (0.59)	1.41 (0.59)
0.25	3.24 (1.02)	1.80 (0.43)	3.00 (0.11)	6.94 (0.25)	1.07 (0.26)	4.95 (0.37)	1.87 (0.38)	4.95 (0.38)	2.89 (0.32)	1.07 (0.26)	6.97 (0.55)	1.80 (0.34)	6.90 (1.34)	1.06 (0.25)	1.06 (0.25)	6.90 (1.34)	1.80 (0.34)	6.90 (1.34)	1.06 (0.25)	1.06 (0.25)
0.2	2.35 (0.52)	1.34 (0.48)	3.00 (0.00)	6.09 (0.28)	1.00 (0.06)	4.27 (0.44)	1.44 (0.50)	4.26 (0.44)	2.33 (0.47)	1.00 (0.07)	6.59 (0.67)	1.34 (0.47)	6.50 (1.11)	1.00 (0.05)	1.00 (0.05)	6.50 (1.11)	1.34 (0.47)	6.50 (1.11)	1.00 (0.05)	1.00 (0.05)
0.15	2.02 (0.15)	1.04 (0.20)	3.00 (0.00)	6.00 (0.00)	1.00 (0.00)	4.00 (0.05)	1.06 (0.24)	4.00 (0.06)	2.01 (0.09)	1.00 (0.00)	5.92 (0.41)	1.04 (0.19)	6.03 (0.36)	1.00 (0.00)	1.00 (0.00)	6.03 (0.36)	1.04 (0.19)	6.03 (0.36)	1.00 (0.00)	1.00 (0.00)
0.1	2.00 (0.00)	1.00 (0.02)	3.00 (0.00)	6.00 (0.00)	1.00 (0.00)	4.00 (0.00)	1.00 (0.04)	4.00 (0.00)	2.00 (0.00)	1.00 (0.00)	5.90 (0.44)	1.00 (0.01)	5.69 (0.72)	1.00 (0.00)	1.00 (0.00)	5.69 (0.72)	1.00 (0.01)	5.69 (0.72)	1.00 (0.00)	1.00 (0.00)
0.05	2.00 (0.00)	1.00 (0.00)	3.00 (0.00)	6.00 (0.00)	1.00 (0.00)	4.00 (0.00)	1.00 (0.00)	4.00 (0.00)	2.00 (0.00)	1.00 (0.00)	5.87 (0.50)	1.00 (0.00)	5.68 (0.73)	1.00 (0.00)	1.00 (0.00)	5.68 (0.73)	1.00 (0.00)	5.68 (0.73)	1.00 (0.00)	1.00 (0.00)

Table 3: The ARL performance of different control charts in Condition III (the corresponding SDRLs are shown in parentheses).

$\mu_{11}$	$(n_1, n_2^{(0)}) = (100, 100)$					$(n_1, n_2^{(0)}) = (100, 500)$					$(n_1, n_2^{(0)}) = (100, 30)$						
	WCSUM	TCUSUM	DTCUSUM	NEWMA	WCSUM	TCUSUM	DTCUSUM	NEWMA	WCSUM	TCUSUM	DTCUSUM	NEWMA	WCSUM	TCUSUM	DTCUSUM	NEWMA	
0.45	199.74	199.62	200.93	199.80	200.59	199.83	200.90	199.42	199.61	199.95	200.69	199.61	199.95	200.69	200.93	197.20	200.70
	(56.66)	(350.33)	(545.96)	(598.43)	(203.57)	(211.44)	(224.29)	(597.55)	(206.64)	(56.45)	(361.23)	(521.66)	(56.45)	(361.23)	(521.66)	(594.93)	(206.61)
0.449	167.71	157.85	203.28	178.40	197.85	163.06	109.78	185.81	194.65	165.72	158.48	211.20	165.72	158.48	211.20	181.20	196.21
	(42.08)	(294.51)	(552.12)	(568.65)	(198.24)	(86.58)	(87.53)	(578.86)	(194.59)	(41.41)	(296.37)	(535.40)	(41.41)	(296.37)	(535.40)	(572.68)	(198.89)
0.448	145.14	121.93	195.60	156.20	176.28	139.61	70.69	157.58	171.14	141.79	120.47	190.07	141.79	120.47	190.07	167.20	173.95
	(32.88)	(229.00)	(545.44)	(535.11)	(168.19)	(46.62)	(45.33)	(536.95)	(160.55)	(31.35)	(224.90)	(513.55)	(31.35)	(224.90)	(513.55)	(552.09)	(170.41)
0.447	121.21	87.90	180.74	129.00	143.18	96.15	46.03	154.94	138.60	117.04	87.07	177.26	117.04	87.07	177.26	130.60	139.76
	(24.92)	(181.44)	(528.30)	(489.53)	(129.68)	(25.75)	(24.75)	(532.85)	(126.64)	(23.21)	(178.39)	(501.38)	(23.21)	(178.39)	(501.38)	(492.37)	(131.72)
0.446	114.27	71.41	170.05	130.80	134.08	41.11	80.22	40.71	136.53	129.67	109.81	182.63	129.67	109.81	182.63	123.40	134.03
	(23.27)	(131.51)	(516.69)	(492.72)	(120.40)	(21.26)	(20.68)	(502.45)	(116.17)	(20.81)	(121.92)	(509.73)	(20.81)	(121.92)	(509.73)	(479.42)	(124.36)
0.445	103.72	55.49	186.70	100.80	116.78	33.47	61.39	33.52	130.73	114.01	98.79	166.77	114.01	98.79	166.77	105.60	116.78
	(19.92)	(91.94)	(542.43)	(435.50)	(103.60)	(15.73)	(15.46)	(492.34)	(100.39)	(17.55)	(88.34)	(488.00)	(17.55)	(88.34)	(488.00)	(445.28)	(105.30)
0.44	72.23	17.70	146.76	48.60	65.71	18.99	17.78	81.06	65.18	66.24	17.62	116.96	66.24	17.62	116.96	51.40	64.22
	(13.38)	(17.88)	(490.49)	(304.87)	(55.57)	(5.99)	(5.99)	(391.93)	(55.04)	(8.96)	(17.70)	(416.90)	(8.96)	(17.70)	(416.90)	(313.48)	(54.93)
0.435	56.77	7.43	82.79	22.00	43.15	12.36	12.31	48.84	42.43	50.56	7.46	7.13	42.43	50.56	7.13	22.00	43.37
	(11.17)	(6.68)	(309.36)	(203.87)	(35.99)	(3.25)	(3.23)	(305.49)	(34.46)	(6.08)	(6.84)	(12.77)	(6.08)	(6.84)	(12.77)	(203.87)	(36.50)
0.43	47.06	3.85	35.99	8.20	30.75	9.70	4.57	20.82	29.95	41.31	3.81	4.10	41.31	3.81	4.10	8.80	30.36
	(10.35)	(3.12)	(136.10)	(119.79)	(25.08)	(2.01)	(2.03)	(198.02)	(24.56)	(4.54)	(3.13)	(4.88)	(4.54)	(3.13)	(4.88)	(124.66)	(24.97)
0.425	40.12	2.39	18.27	3.80	23.43	8.16	8.16	12.21	23.50	35.04	2.37	3.08	35.04	2.37	3.08	4.40	23.17
	(9.46)	(1.69)	(76.03)	(74.78)	(19.23)	(1.40)	(2.06)	(149.25)	(19.50)	(3.65)	(1.65)	(2.86)	(3.65)	(1.65)	(2.86)	(82.40)	(19.22)
0.42	34.28	1.72	9.87	1.20	18.98	7.20	2.05	6.60	18.72	30.48	1.70	2.52	30.48	1.70	2.52	1.60	18.63
	(8.73)	(1.00)	(45.56)	(20.00)	(15.65)	(1.04)	(1.27)	(105.69)	(15.97)	(2.88)	(1.00)	(1.75)	(2.88)	(1.00)	(1.75)	(34.64)	(15.45)
0.415	29.06	1.35	5.78	1.40	15.67	6.52	1.59	4.00	15.34	27.11	1.36	2.24	27.11	1.36	2.24	1.40	15.57
	(7.49)	(0.63)	(28.39)	(28.28)	(13.35)	(0.80)	(0.84)	(77.41)	(13.03)	(2.46)	(0.65)	(1.08)	(2.46)	(0.65)	(1.08)	(28.28)	(13.44)
0.41	24.72	1.17	4.04	1.20	13.15	6.02	1.33	6.03	12.92	24.48	1.17	2.10	24.48	1.17	2.10	1.00	13.00
	(5.38)	(0.42)	(19.05)	(20.00)	(11.33)	(0.66)	(0.60)	(44.71)	(11.17)	(2.11)	(0.42)	(0.65)	(2.11)	(0.42)	(0.65)	(11.40)	(11.40)
0.405	21.65	1.07	2.66	1.00	11.13	5.68	1.18	5.67	10.98	22.33	1.07	2.04	22.33	1.07	2.04	1.00	11.11
	(3.31)	(0.27)	(10.07)	(0.00)	(9.76)	(0.59)	(0.42)	(44.71)	(9.64)	(1.85)	(0.27)	(0.37)	(9.64)	(1.85)	(0.37)	(0.00)	(9.89)
0.4	19.60	1.03	2.25	1.00	9.74	5.37	1.08	5.37	9.58	20.56	1.03	2.01	20.56	1.03	2.01	1.00	9.74
	(1.82)	(0.17)	(5.85)	(0.00)	(8.70)	(0.51)	(0.29)	(20.00)	(8.61)	(1.59)	(0.16)	(0.23)	(8.61)	(1.59)	(0.23)	(0.00)	(8.68)
0.35	12.14	1.00	2.00	1.00	3.68	2.29	1.00	2.28	3.59	12.53	1.00	2.00	12.53	1.00	2.00	1.00	3.65
	(0.55)	(0.00)	(0.00)	(0.00)	(3.70)	(0.58)	(0.57)	(0.00)	(3.63)	(0.58)	(0.00)	(0.00)	(3.63)	(0.58)	(0.00)	(0.00)	(3.63)
0.3	9.65	1.00	2.00	1.00	2.02	2.00	1.00	2.00	2.05	9.95	1.00	2.00	2.05	1.00	2.00	1.00	2.07
	(0.48)	(0.00)	(0.00)	(0.00)	(2.02)	(0.00)	(0.00)	(0.00)	(2.13)	(0.31)	(0.00)	(0.00)	(2.13)	(0.31)	(0.00)	(0.00)	(2.17)
0.25	8.14	1.00	2.00	1.00	1.47	2.00	1.00	2.00	1.46	8.72	1.00	2.00	1.46	1.00	2.00	1.00	1.47
	(0.35)	(0.00)	(0.00)	(0.00)	(1.37)	(0.00)	(0.00)	(0.00)	(1.32)	(0.45)	(0.00)	(0.00)	(1.32)	(0.45)	(0.00)	(0.00)	(1.34)
0.2	7.54	1.00	2.00	1.00	1.25	2.00	1.00	2.00	1.23	7.96	1.00	2.00	1.23	1.00	2.00	1.00	1.27
	(0.50)	(0.00)	(0.00)	(0.00)	(1.02)	(0.00)	(0.00)	(0.00)	(0.93)	(0.19)	(0.00)	(0.00)	(0.93)	(0.19)	(0.00)	(0.00)	(1.07)
0.15	7.00	1.00	2.00	1.00	1.16	2.00	1.00	2.00	1.15	7.02	1.00	2.00	1.15	1.00	2.00	1.00	1.15
	(0.05)	(0.00)	(0.00)	(0.00)	(0.77)	(0.00)	(0.00)	(0.00)	(0.74)	(0.14)	(0.00)	(0.00)	(0.74)	(0.14)	(0.00)	(0.00)	(0.79)
0.1	6.86	1.00	2.00	1.00	1.13	2.00	1.00	2.00	1.10	7.00	1.00	2.00	1.10	1.00	2.00	1.00	1.11
	(0.35)	(0.00)	(0.00)	(0.00)	(0.67)	(0.00)	(0.00)	(0.00)	(0.59)	(0.04)	(0.00)	(0.00)	(0.59)	(0.04)	(0.00)	(0.00)	(0.62)
0.05	6.00	1.00	2.00	1.00	1.09	2.00	1.00	2.00	1.09	6.87	1.00	2.00	1.09	1.00	2.00	1.00	1.09
	(0.02)	(0.00)	(0.00)	(0.00)	(0.54)	(0.00)	(0.00)	(0.00)	(0.54)	(0.34)	(0.00)	(0.00)	(0.54)	(0.34)	(0.00)	(0.00)	(0.56)

model is considered: the  $\mathcal{P}^{(t)}$  ( $t = 1, 2, \dots$ ) follow the model in Equation (12), while the  $(n_1^{(t)}, n_2^{(t)})$  ( $t = 1, 2, \dots$ ) comes from the model in Equation (13). Then let  $n_{ij}^{(t)} \sim \text{multinomial}(n_i^{(t)}; p_{ij})$  ( $i, j = 1, 2$ ).

The values of ARLs and SDRLs when the initial total numbers of transition are equal to (100, 500) are visualized in Figures 4. The more similar results when  $(n_1^{(0)}, n_2^{(0)}) = (100, 100)$  and  $(n_1^{(0)}, n_2^{(0)}) = (100, 30)$  are available upon request. From Figures 4, we can see that:

- The TCUSUM control chart is most sensitive in this case with the smallest ARLs. The WSCUSUM and NEWMA control charts behave similarly with their own specialty. The WSCUSUM performs better than NEWMA when shifts are slightly large and vice-versa. The DTCUSUM and DTCUSUM-n control charts are the worst, with the largest and nonmonotonic ARLs.
- The WSCUSUM and NEWMA control charts are the two most robust of the five control charts since the SDRLs of them are the smallest. Though the TCUSUM control chart has the smallest ARLs, its robustness is worst with the largest SDRLs. It noticed that the value of SDRL is almost three times larger than that of ARL. The big values of SDRLs in the DTCUSUM and DTCUSUM-n control charts are not to be lightly ignored.

To sum up, the WSCUSUM and NEWMA control charts are better ones when the total number and probability of transition are both serially correlated, with the comparatively small ARLs and SDRLs at the same time. The former performs better when the shifts are large, while the latter behaves better when the shifts are small.

### 3.3 The performance in the case of correlated row data

In this subsection, we discuss a much more complex and realistic case, that is the  $\mathcal{P}_1^{(t)}$  and  $\mathcal{P}_2^{(t)}$  are correlated. To describe this feature, we assume the following model:

$$\begin{aligned} p_{11}^{(t)} &= \min \left( 1, \left( 0.5p_{11}^{(t-1)} + 0.5\underline{\epsilon}_1^{(t)} \right) \vee 0 \right), \\ p_{22}^{(t)} &= \min \left( 1, \left( 0.9p_{11}^{(t-1)} + 0.1\underline{\epsilon}_2^{(t)} \right) \vee 0 \right), \end{aligned} \tag{14}$$

where  $\underline{\epsilon}_1^{(t)}$  and  $\underline{\epsilon}_2$  ( $t = 1, 2, \dots$ ) are i.i.d. with the distribution  $N(p_{11}^{(t-1)}, 0.0001)$ . Then  $p_{12}^{(t)} = 1 - p_{11}^{(t)}$  and  $p_{21}^{(t)} = 1 - p_{22}^{(t)}$ . Similarly,  $(n_1^{(t)}, n_2^{(t)})$  ( $t = 1, 2, \dots$ ) comes from the model in Equation (13) and

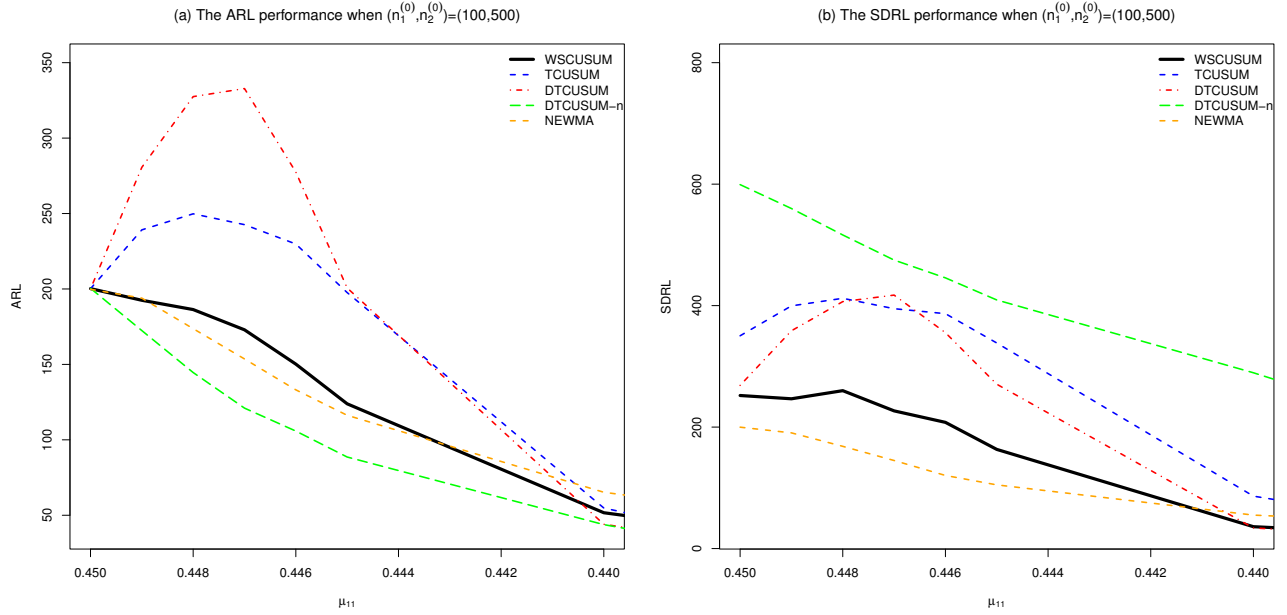


Figure 4: The performance of different control charts when the total number and probability of transition are both serially correlated.

$$n_{ij}^{(t)} \sim \text{multinomial}(n_i^{(t)}; p_{ij}) \quad (i, j = 1, 2).$$

Figure 5 displays that our novel approach is the most robust with the smallest SDRLs. The SDRLs of the other four charts are much larger than their ARLs, especially when the shifts are small. Though our method is not the most sensitive one when shifts are small, it behaves the best when the shifts are slightly large and also has an acceptable performance when shifts are small. Finally, compared with the results in Section 3.1 and Section 3.2, the more complex the networks, the more obvious the advantages of the WSCUSUM control chart.

## 4 Metro traffic example revisited

Traffic online monitoring is crucial for the operating managers to make appropriate evaluations of the real line health and plan for the next. In this subsection, the example mentioned in the Introduction is revisited to demonstrate the application of the proposed control chart.

The data set is drawn from a big data platform for smart transportation applications, including the user ID, ticket records, transaction time, in-gate/out-gate station and so on. Table 4 displays a few sample rows of the data collected from the big data platform. Considering the operator's requirements for monitoring, the amount of transactions per half hour is used in detecting abnormal

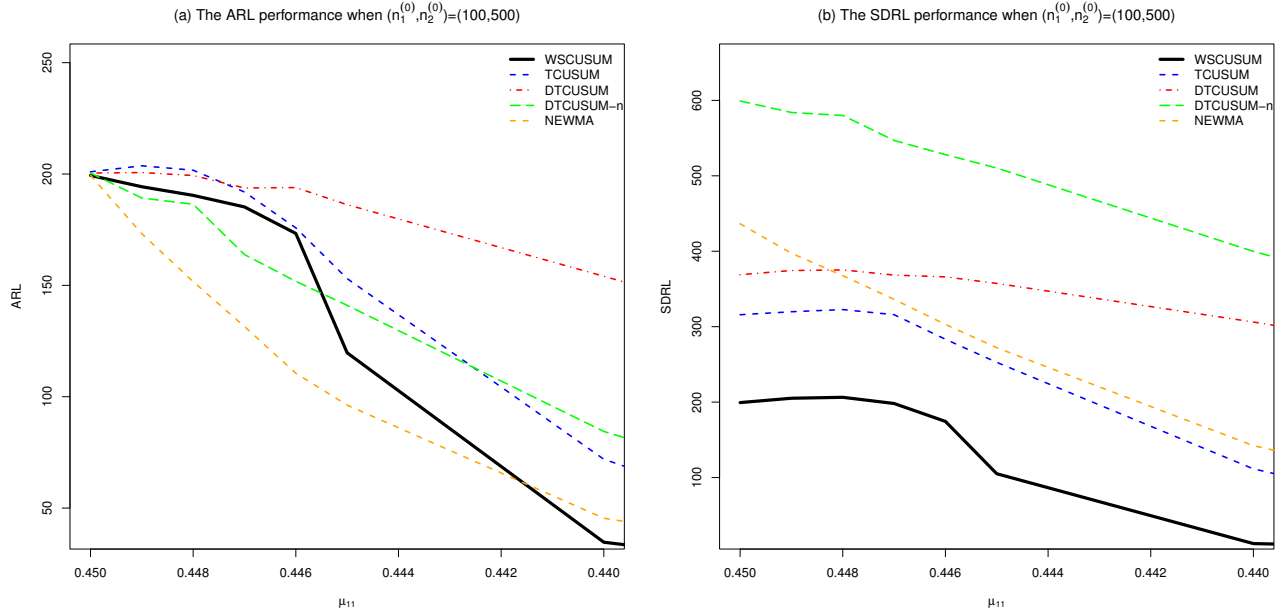


Figure 5: The performance of different control charts when the total number and probability of transition are both serially correlated and row data are correlated.

behavior. We detect the traffic problem in a certain line, that consists of fourteen stations, from 06:00 to 23:30 every day and the data analysis proceeds in several steps as follows:

- **Step 1: Traffic measurement.**

At the ending of every half hour, the amount of transition from one station to another station is counted and the matrix  $\mathcal{N}^{(t)}$  is obtained. Data management is then performed and we get the  $\mathcal{P}^{(t)}$ .

- **Step 2: Phase I establishment.**

Actually, the company meets a big traffic problem in 2019 because of some social events. In this paper, the records in 2017 are chosen to form Phase I (the in-control stage). We use the first eleven months' data to estimate some parameters, such as mean vector, covariance matrix, correlation coefficient and control limits. Guided by the data provider, the value of  $B_{max}$  is equal to four here, which means that the past observations beyond the 2 hours of the current time provide little useful information. By the way, we assume that the  $ARL_0 = 200$  same as the fact that a false alarm would be given weekly in the in-control process. The control limits of the five control charts mentioned in Section 3 are shown in Table 5.

Table 4: The samples of the traffic data collected from the big data platform.

Octopus ID	Transaction Time	Transaction Type	In-gate Station	Out-gate Station	Train Direction	Fare
900125532	2012/12/31 18:27	ENT	29	29	1	0
900125532	2012/12/31 18:47	USE	29	49	2	10.5
900125582	2012/12/31 18:18	ENT	27	27	1	0
900125582	2012/12/31 18:44	USE	27	48	2	10.5
900125585	2012/12/31 6:45	ENT	49	49	1	0
900125585	2012/12/31 7:24	USE	49	97	2	9.7
900125600	2012/12/31 19:07	ENT	6	6	1	0
900125600	2012/12/31 19:14	USE	6	18	2	4.9
900125603	2012/12/31 10:52	ENT	6	6	1	0
900125603	2012/12/31 11:02	USE	6	3	2	4.9

Table 5: Control limits of real-data example

Control charts	WSCUSUM	TCUSUM	DCUSUM	DCUSUM-n	NEWMA
h/L	638.5	62.63	18300	0.28	17.26

- **Step 3: Phase I back-testing.**

Intuitively, the situation of serial correlation raises the false alarm rate of the conventional control charts. To demonstrate the robustness of our proposed WSCUSUM control chart, we test the five control ones in IC data from December 7 to December 13 in 2017. Figure 6 shows that the conventional control charts without de-correlation (e.g., TCUSUM and NEWMA ones) both alert, while the WSCUSUM and DCUSUM do not make the false. As for the DCUSUM-n control chart, it only gives a signal at the 1-st observation. Thus the detection of transition number matrix does not work in a complex directed network. In this way, we conclude that our model performs more robustly compared with the others.

- **Step 4: Phase II monitoring.**

In this step, we monitor the OC data from November 11 to November 15 in 2019 to display the sensitivity of our proposed WSCUSUM control chart. As Figure 7 illustrated, the WSCUSUM and TCUSUM control charts signal at the 4-th observation. Slightly later, the DCUSUM control ones signal at the 19-th observation. As for the DCUSUM-n and NEWMA control chart, the cumulative statistics do not increase with the persistent shifts. Thus, our method is most effective in Phase II.

Above all, the proposed WSCUSUM scheme performs more robustly and sensitively.

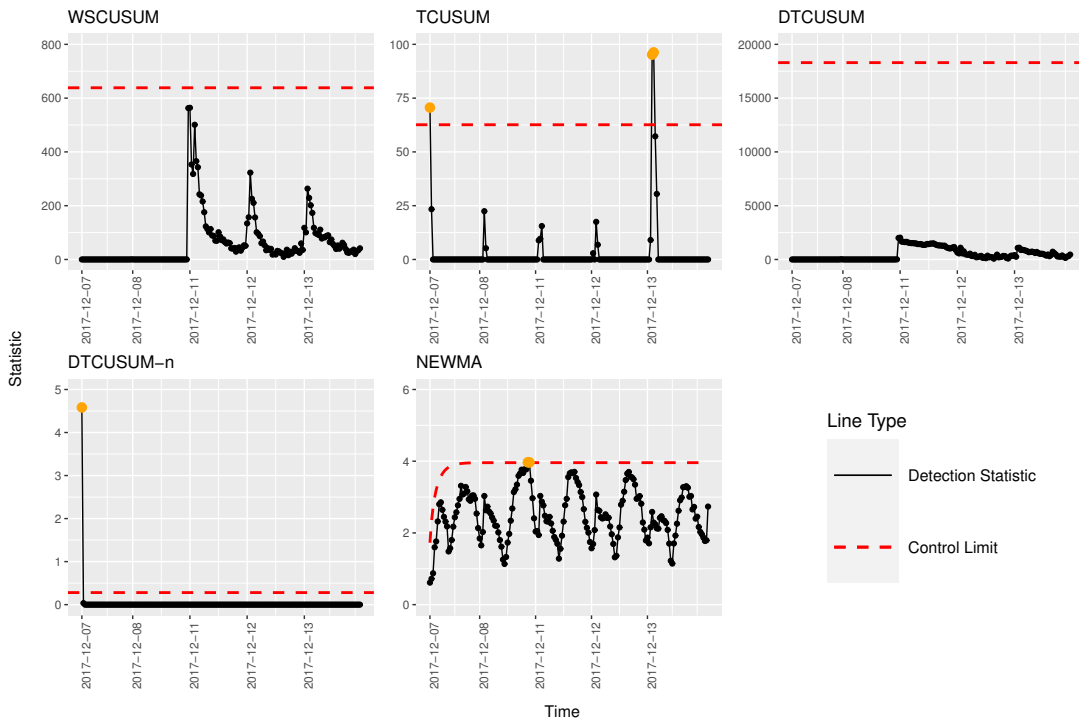


Figure 6: Phase I back-testing performances of five models

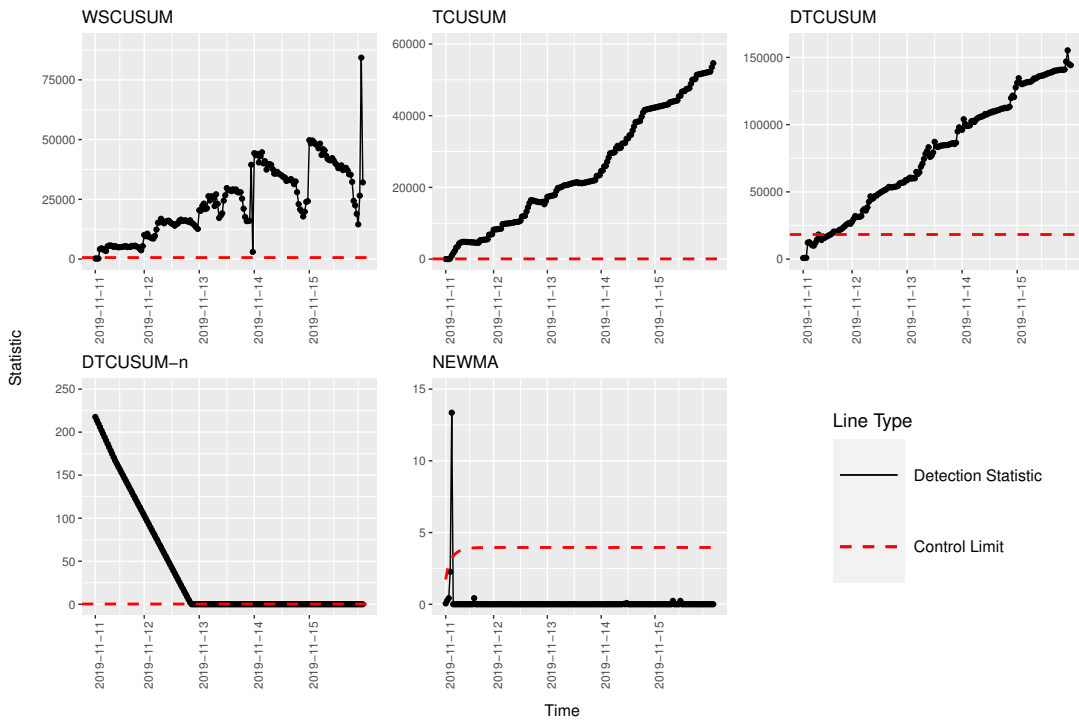


Figure 7: Phase II performance of five models

## 5 Conclusion

In this paper, prompted by an interesting real metro traffic detection, we propose an innovative weighted CUSUM control chart with the spring-length-based de-correlation approach to monitor the serially correlated directed networks. The dynamic features are common in real applications, especially when the time difference between the two adjacent points is small. Moreover, in a network, the doubly serial correlation of the transition numbers, makes the problem more complex. Thus we propose to detect the shifts in the transition probability matrix rather than the transition matrix to improve the robustness of the algorithm. And we extend the spring-length-based de-correlation approach without any parametric assumptions to the multivariate vectors and design independent test statistics. Finally, in consideration of the importance of nodes, a weighted CUSUM control scheme is suggested, in which we regard the total numbers of transitions in each node as the weighting function. Both simulation results and a real-data example of monitoring the mean shifts in the metro traffic illustrate that our method is much robust and sensitive, in particular the SDRs are always small enough. In summary, our charting method is a powerful tool for many process monitoring applications because of its great flexibility.

In the end, we think there still are lots of new opportunities for research into approaches to robust and sensitive monitoring algorithms in serially correlated networks. On the one hand, much big sample size is required in estimating the  $\gamma(B)$  ( $B \leq B_{max}$ ) especially when the value of  $B_{max}$  and the number of nodes are large. The much practical de-correlation method in the case where IC sample size  $m$  is small will be developed in further research. On the other hand, though we mainly focus on the case of small shift detection, we have to admit that our method is not as sensitive as the traditional control charts in large shift monitoring. An improved method that strikes a balance between robustness and sensitivity in the case of complex serial correlation can be considered.

## References

- Apley D.W., and Shi, J. (1999). The GLRT for statistical process control of autocorrelated processes. *IIE Transactions*, 31, 1123-1134.
- Asikainen, A., Iñiguez, G., Ureña-Carrión, G., Kaski, K., and Kivelä, M. (2020). Cumulative effects of triadic closure and homophily in social networks. *Science Advances*, 6(19): eaax7310.

- Azarnoush, B., Paynabar, K., Bekki, J., and Runger, G. (2016). Monitoring temporal homogeneity in attributed network streams. *Journal of Quality Technology*, 48(1), 28-43.
- Campion, G., Van Breusegem, V., Pinson, P., and Bastin, G. (1985). Traffic regulation of an underground railway transportation system by state feedback. *Optimal Control Applications and Methods*, 6(4), 385-402.
- Chatterjee, S., and Qiu, P. (2009). Distribution-free cumulative sum control charts using bootstrap-based control limits. *The Annals of Applied Statistics*, 3, 349-369.
- Chen, R., Xiao, H., and Yang, D. (2021). Autoregressive models for matrix-valued time series. *Journal of Econometrics*, 222, 539-560.
- Chenouri, S., Steiner, S.H., and Variyath, A.M. (2009). A multivariate robust control chart for individual observations. *Journal of Quality Technology*, 41, 259-271.
- Chunaev, P. (2020). Community detection in node-attributed social networks: A survey. *Computer Science Review*, 37, 100286
- Crane, H., and Dempsey, W. (2018). Edge exchangeable models for interaction networks. *Journal of the American Statistical Association*, 113(523), 1311-1326.
- Fang, Q., and Huang, S. (2013). A directed network analysis of heterospecific pollen transfer in a biodiverse community. *Ecology*, 94(5), 1176-1185.
- Gao, Z., and Jin, N. (2012). A directed weighted complex network for characterizing chaotic dynamics from time series. *Nonlinear Analysis: Real World Applications*, 13(2), 947-952.
- Han, D., Tsung, F., Xian, J., and Yu, M. (2020). Optimal sequential tests for monitoring changes in the distribution of finite observation sequences. *Statistica Sinica*, doi: 10.5705/ss.202020.0333.
- Harris, T.J., and Ross, W.H. (1991). Statistical process control procedures for correlated observations. *The Canadian Journal of Chemical Engineering*, 69(1), 48-57.
- Kilduff, M., and Tsai, W. (2003). *Social networks and organizations*. London, UK: Sage.
- Li, J., and Qiu, P. (2016). Nonparametric dynamic screening system for monitoring correlated longitudinal data. *IIE Transactions*, 48(8), 772-786.

- Li, W., and Qiu, P. (2020). General charting scheme for monitoring serially correlated data with short-memory dependence and nonparametric distributions. *newblock IISE Transactions*, 52(1), 61-74.
- Li, Y., and Tsung, F. (2009). False discovery rate-adjusted charting schemes for multistage process monitoring and fault identification. *Technometrics*, 51(2), 186-205.
- Li, S., Yang, L., Gao, Z., and Li, K. (2016). Robust train regulation for metro lines with stochastic passenger arrival flow. *Information Sciences*, 37, 287-307.
- Lin, W.S., and Sheu, J.W. (2010). Automatic train regulation for metro lines using dual heuristic dynamic programming. *Proceedings of the Institution of Mechanical Engineers, Part F*, 224(1), 15-23.
- Loredo, E., Jearekpor, D., and Borrer, C. (2002), Model-based control chart for autoregressive and correlated data. *Quality and Reliability Engineering International*, 18, 489-496.
- McCulloh, I., and Carley, K.M. (2011). Detecting change in longitudinal social networks. *Journal of Social Structure*, 12, 1-37.
- Mei, Y. (2010). Efficient scalable schemes for monitoring a large number of data streams. *Biometrika*, 97(2), 419-433.
- Page, E.S. (1954). Continuous inspection scheme. *Biometrika*, 41, 100-114.
- Perry, M.B. (2020). An EWMA control chart for categorical processes with applications to social network monitoring. *Journal of Quality Technology*, 52(2), 182-197.
- Qiu, P., Li, W., and Li, j. (2020) A new process control chart for monitoring short-range serially correlated data. *Technometrics*, 62(1), 71-83.
- Qiu, P., and Xiang, D. (2014). Univariate dynamic screening system: An approach for identifying individuals with irregular longitudinal behavior. *Technometrics*, 56, 248-260.
- Qiu, P., and Xie, X. (2021). Transparent sequential learning for statistical process control of serially correlated data. *Technometrics*, doi: 10.1080/00401706.2021.1929493.

- Roberts, S.W. (1959). Control charts tests based on geometric moving average. *Technometrics*, 42, 97-101.
- Schmid, W., and A. Schöne. (1997). Some properties of the EWMA control chart in the presence of autocorrelation. *The Annals of Statistics*, 25(3), 1277-1283.
- Shewhart, W.A. (1925). The application of statistics as an aid in maintaining quality of a manufactured product. *Journal of the American Statistical Association*, 20, 546-548.
- Umakanth, B., and Damodhar, J. (2013). Detection of energy draining attack using EWMA in wireless Ad Hoc sensor networks. *International Journal of Engineering Trends and Technology*, 4, 3691-3695.
- Vargas, J.A. (2003). Robust estimation in multivariate control charts for individual observations. *Journal of Quality Technology*, 35, 367-376.
- Wang, Z., Wu, C., Yu, M., and Tsung, F. (2021). Self-starting process monitoring based on transfer learning. *Journal of Quality Technology*, doi: <https://doi.org/10.1080/00224065.2021.1991251>.
- Woodall, W.H., Zhao, M.J., Paynabar, K., Sparks, R., and Wilson, J.D. (2017). *An overview and perspective on social network monitoring*. *IISE Transactions*, 49(3), 354-365.
- Xiang, D., Li, W., Tsung, F., Pu, X., and Kang, Y. (2021). Fault classification for high-dimensional data streams: A directional diagnostic framework based on multiple hypothesis testing. *Naval Research Logistics*, 68(7): 973-987.
- Xue, L., and Qiu, p. (2021). A nonparametric CUSUM chart for monitoring multivariate serially correlated processes. *Journal of Quality Technology*, 53(4), 396-409.
- Yu, M., Wu, C., and Tsung, F. (2019). Monitoring the data quality of data streams using a two-step control scheme. *IISE Transactions*, 51(9), 985-998.
- Yu, M., Wu, C., and Tsung, F. (2021). Change detection in parametric multivariate dynamic data streams using the ARMAX-GARCH model. *Journal of Quality Technology*, doi: <https://doi.org/10.1080/00224065.2021.1903820>.

- Yu, J., Xie, W., and Jiang, Z. (2018). Early warning model based on correlated networks in global crude oil markets. *Physica A: Statistical Mechanics and its Applications*, 490, 1335-1343.
- Zhang, Z., Delplace, P., and Fleury, R. (2021). Superior robustness of anomalous non-reciprocal topological edge states. *Nature*, 598, 293-297.
- Zou, C., Wang, G., and Li, R. (2020). Consistent selection of the number of change-points via sample-splitting. *The Annals of Statistics*, 48(1), 413-439.